Program: Radar and Satellite Meteorology

Research Highlights

Assessment of Satellite Measurements over Indian sub-continent

Performance of Global Precipitation Measurement (GPM) estimates

➢ Rainfall products from GPM, especially the Integrated Multi-satellitE Retrievals for the GPM (IMERG) is assessed using ground-based observations (rain gauge and Joss-Waldvogel Disdrometer; JWD) and TRMM measurements

➢ Comparison period: June-September, 2014

Comparison of GPM measurements with Rain gauge, JWD and TRMM:

❑ IMERG rainfall data are compared with six rain gauge measurements over Western Ghats (Ambeghar, Jor, Khengarewadi, Medha, Velhe and Wathar)
❑ IMERG rain rates are compared with JWD and TRMM measurements at High Altitude Cloud Physics Laboratory (HACPL) in Mahabaleswar.
❑ The drop size distribution (DSD) measurements between GPM and JWD are also evaluated.

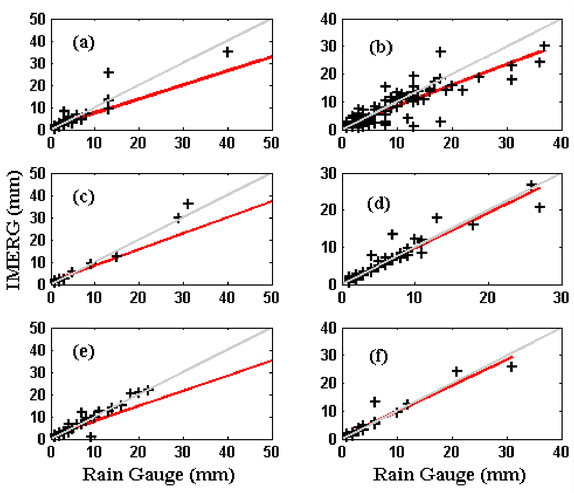

Comparison of accumulated rain between IMERG and rain gauge

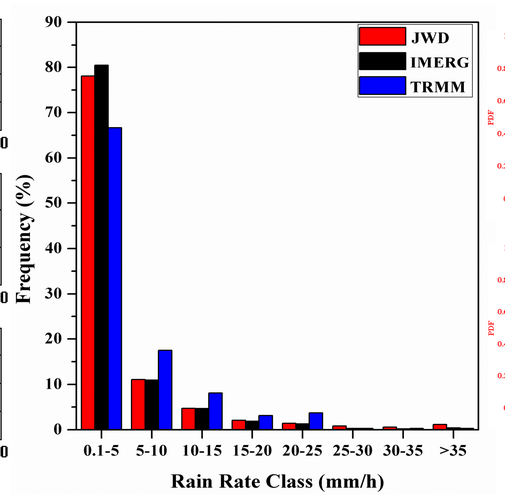

Frequency distribution of rain rates

Distribution of D_m and N_w

❖ IMERG shows good agreement with rain gauge measurements, however it underestimates the measured rainfall.
❖ IMERG rainfall product shows better measurements in light precipitation events (0-5 mm/h) compared to TRMM measurements.
❖GPM underestimates the mean D_m and overestimates the mean N_w compared to JWD.

Diurnal variation of rainfall revealed from IMERG:

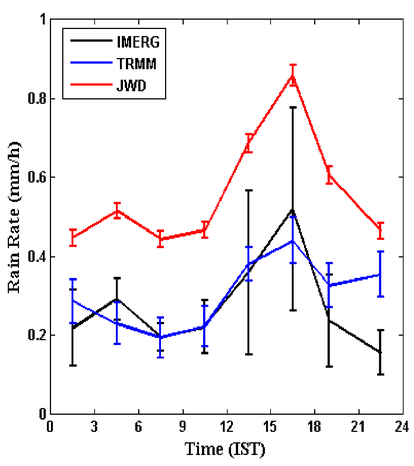

Diurnal variation of rain rates over HACPL

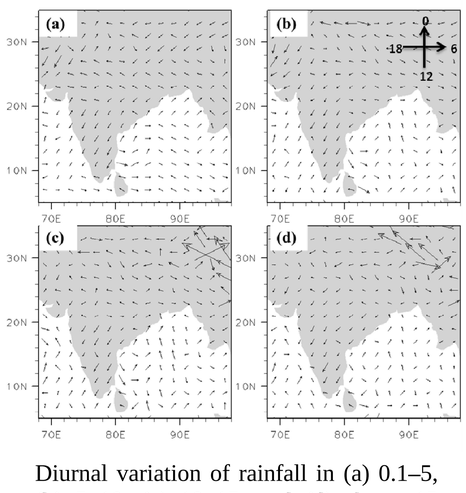

Diurnal variation of rainfall in (a) 0.1–5, (b) 5–10, (c) 10–15, and (d) above 15 mm/h rain rates from IMERG

✓ IMERG captures the occurrence of maximum rain rates .

✓ The secondary maximum in observed rain rate is well represented in IMERG measurements.

✓ The amplitude (length of the arrow) and phase (arrow) of the diurnal component of rainfall shows distinct spatial variability over land and oceans.

✓ The rainfall peaks in the morning (0400–0500 LT) over oceans and between afternoon and evening hours in most of the land regions.

Spatial distribution of rainfall from TRMM and IMERG:

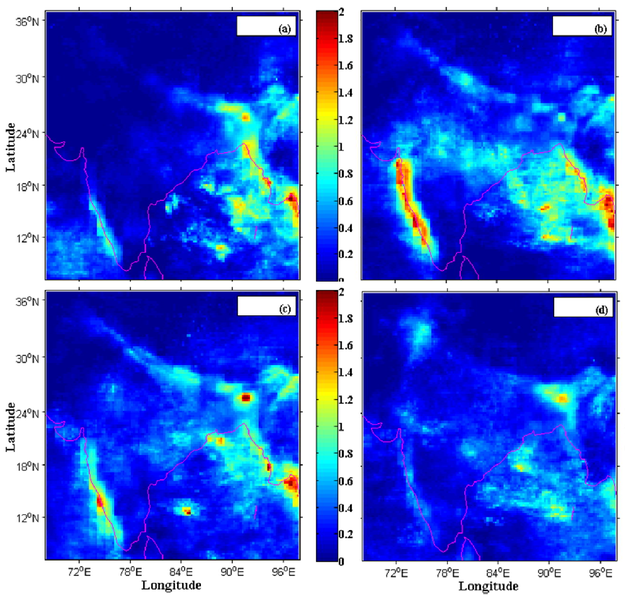

Monthly mean rain rate (a) June, (b) July, (c) August, and (d) September from TRMM

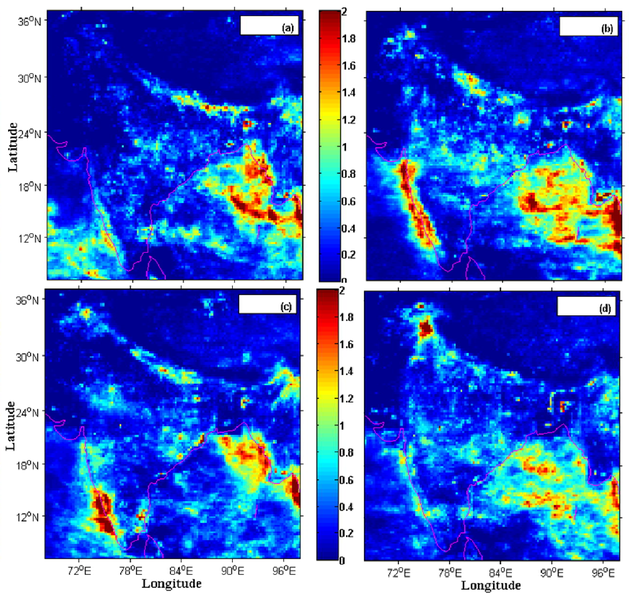

Monthly mean rain rate (a) June, (b) July, (c) August, and (d) September from IMERG

❖The spatial distribution of large scale rainfall patterns are well represented by IMERG.
❖ The orographic precipitation over the foothills of Himalayas and West coast of India is well captured in IMERG measurements.
❖ However, the IMERG overestimated the rainfall over regions of heavy rainfall and mountainous regions.
❖ Overall, this preliminary accuracy assessment highlights that the IMERG product can adequately substitute the TRMM-3B42 products.
❖ The analysis of the GPM constellation satellite-based rainfall estimates reported here can give the satellite precipitation users a better understanding of the features associated with currently available IMERG precipitation estimates

Murali Krishna et al., (2017), *Earth SP. Sci.*

Estimation and evaluation of CAPE from INSAT-3D measurements

CAPE is estimated from high-resolution geostationary INSAT-3D measurements

$$CAPE = \int_{LFC}^{EL} \left(\frac{g(T_{vp} - T_{ve})}{T_{ve}} \right) dz$$

❖ Comparison period: April, 2014-March, 2017

Evaluation of INSAT-3D CAPE with Radiosonde and ERA-interim:

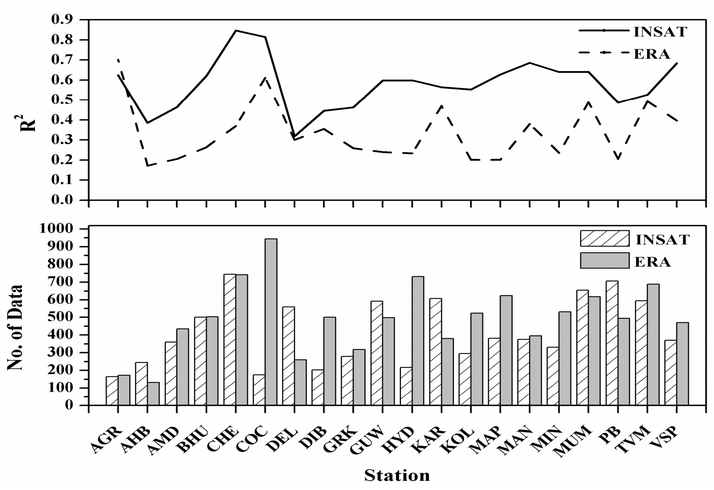

Correlation coefficient and population in the comparison of INSAT-3D and ERA CAPE with radiosonde derived CAPE

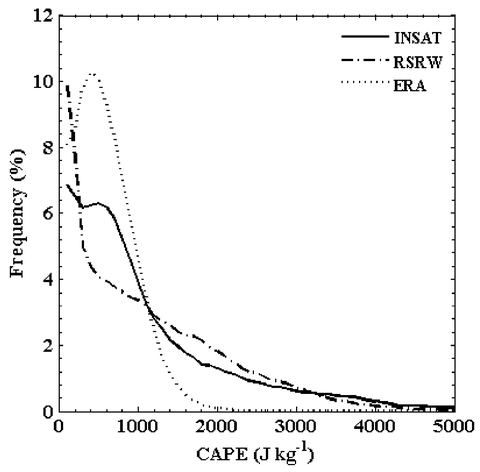

Distribution of INSAT-3D, radiosonde and ERA reanalysis CAPE

❖ For the first time, CAPE is estimated from INSAT-3D measurements and are evaluated using radiosonde measurements.
❖ INSAT-3D estimates are superior to ERA reanalysis estimates.
❖ The distribution of CAPE is shifted to lower values in all the three measurements.
❖The INSAT-3D estimated CAPE matches well with the radiosonde measurements above ~3000 J/kg.

Spatial distribution of INSAT-3D CAPE:

❖ To observe the spatial distribution of extreme weather events, the estimated CAPE is divided into four categories: weak instability (<500 J/kg), moderate instability (501-1500 J/kg), strong instability (1501-3000 J/kg), and extreme instability (>3000 J/kg).

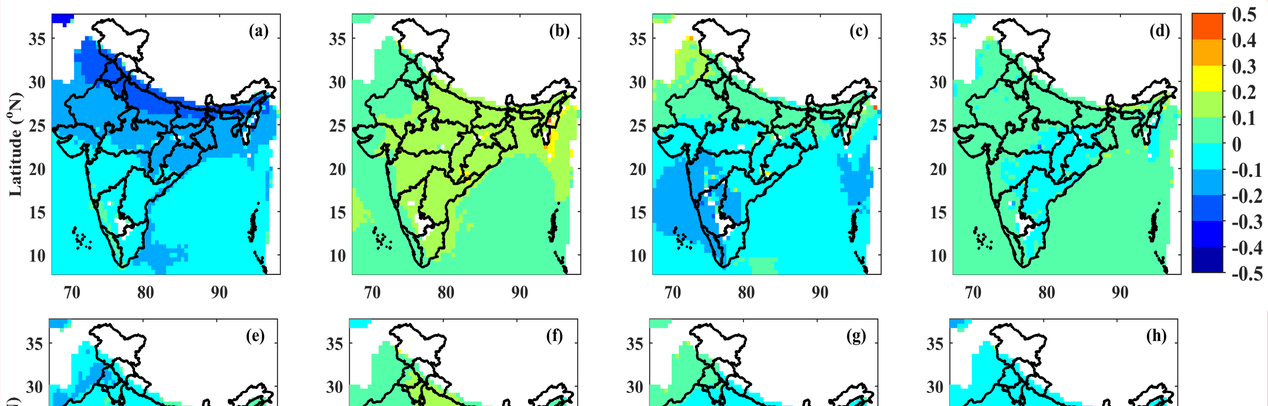

The normalized anomaly distribution of CAPE in the four instability conditions during (a)-(d) winter, (e)-(h) pre-monsoon, (i)-(l) monsoon and (m)-(p) post-monsoon seasons

➢ Weak instability is predominant during winter, moderate instability is higher during post-monsoon, strong instability is more during monsoon and extreme instability is higher during pre-monsoon season.

Diurnal variation of CAPE over different regions:

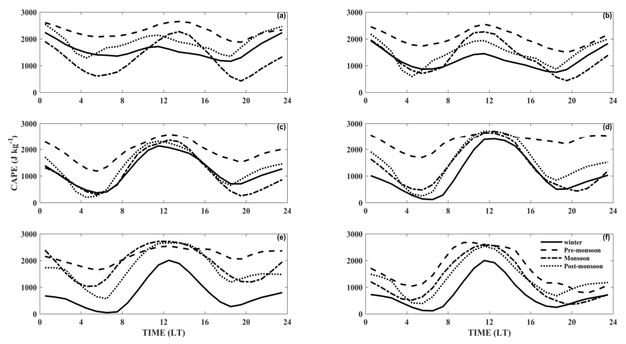

❖To observe the diurnal variation of CAPE over different parts of India, the study region is divided (latitude-wise for uniformity) into six sub-regions, the Arabian Sea, Bay of Bengal, South Peninsular India, Central India, North India and Northeast India.

❖The diurnal variation in mean CAPE shows a bi-modal distribution with primary peak around mid-night and secondary peak in the afternoon.

Murali Krishna et al. (under review)

We acknowledge to JAXA JAPAN, NASA USA, SAC ISRO and University of Wyoming for the provision of GPM, TRMM, INSAT-3D and Radiosonde data sets.